

ORIGINAL ARTICLE

HEPATOLOGY

HIGHLIGHTS

- Changes in the composition of the intestinal microbiota are related to the development of alcoholic liver disease and metabolic-dysfunction associated steatotic liver disease.
- The diversity of the intestinal microbiota was lower in animals with MASLD compared to ALD.
- The structural pattern of the intestinal microbiota was significantly different among the experimental groups.
- Studies are needed to characterize the composition of the intestinal microbiota and metabolome to find new therapeutic strategies.

Received: 7 July 2023
Accepted: 30 August 2023

Declared conflict of interest of all authors: none
Disclosure of funding: This study was supported by the following Brazilian funding agencies: National Council for Scientific and Technological Development, CNPq; Coordination for the Improvement of Higher Education Personnel, CAPES/PNPD and Research Incentive Fund from Hospital de Clínicas de Porto Alegre, FIPE-HCPA.
Declaration of use of artificial intelligence: none
Corresponding author: Mário Reis Álvares-da-Silva.
E-mail: marioreis@live.com



doi.org/10.1590/S0004-2803.24612023-100

Comparison of gut microbiota in alcoholic and metabolic-dysfunction associated steatotic liver disease in animal models

Cássio Marques **PERLIN**^{1,2}, Larisse **LONGO**^{1,2}, Rutiane Ullmann **THOEN**^{1,2}, Carolina **URIBE-CRUZ**^{1,2,3} and Mário Reis **ÁLVARES-DA-SILVA**^{1,2,4,5}

¹ Universidade Federal do Rio Grande do Sul, Programa de Pós-Graduação em Gastroenterologia e Hepatologia, Porto Alegre, RS, Brasil. ² Hospital de Clínicas de Porto Alegre, Laboratório Experimental de Hepatologia e Gastroenterologia, Centro de Pesquisa Experimental, Porto Alegre, RS, Brasil. ³ Universidade Católica de las Misiones, Posadas – 3300, Misiones, Argentina.

⁴ Hospital de Clínicas de Porto Alegre, Divisão de Gastroenterologia, Porto Alegre, RS, Brasil.

⁵ Pesquisador do Conselho Nacional de Desenvolvimento Científico e Tecnológico, CNPq, Brasil.

ABSTRACT – Background – Alcoholic liver disease (ALD) and metabolic-dysfunction associated steatotic liver disease (MASLD) are common, and gut microbiota (GM) is involved with both. Here we compared GM composition in animal models of MASLD and ALD to assess whether there are specific patterns for each disease. **Methods** – MASLD model— adult male Sprague Dawley rats, randomized into two groups: MASLD-control (n=10) fed a standard diet; MASLD-group (n=10) fed a high-fat-choline-deficient diet for 16 weeks. ALD model— adult male Wistar rats randomized: ALD-control (n=8) fed a standard diet and water+0.05% saccharin, ALD groups fed with sunflower seed and 10% ethanol+0.05% saccharin for 4 or 8 weeks (ALC4, n=8; ALC8, n=8). ALC4/8 on the last day received alcoholic binge (5g/kg of ethanol). Afterwards, animals were euthanized, and feces were collected for GM analysis. **Results** – Both experimental models induced typical histopathological features of the diseases. Alpha diversity was lower in MASLD compared with ALD ($p<0.001$), and structural pattern was different between them ($P<0.001$). *Bacteroidetes* (55.7%), *Firmicutes* (40.6%), and *Proteobacteria* (1.4%) were the most prevalent phyla in all samples, although differentially abundant among groups. ALC8 had a greater abundance of the phyla *Cyanobacteria* (5.3%) and *Verrucomicrobiota* (3.2%) in relation to the others. Differential abundance analysis identified *Lactobacillaceae_unclassified*, *Lachnospiraceae_NK4A136_group*, and *Turicibacter* associated with ALC4 and the *Clostridia_UCG_014_ge* and *Gastranaerophilales_ge* genera to ALC8. **Conclusion** – In this study, we demonstrated that the structural pattern of the GM differs significantly between MASLD and ALD models. Studies are needed to characterize the microbiota and metabolome in both clinical conditions to find new therapeutic strategies.

Keywords – Animal model; alcoholic liver disease; gut microbiota; metabolic-dysfunction associated steatotic liver disease; liver disease.

INTRODUCTION

Metabolic-dysfunction associated steatotic liver disease (MASLD), the current terminology for non-alcoholic fatty liver disease, and alcoholic liver disease (ALD) are two major types of chronic liver disease worldwide^(1,2). Although there are some differences in hepatotoxicity caused by excess caloric intake versus heavy alcohol consumption, both share genetic and epigenetic risk factors, systemic inflammation, and histopathological findings^(1,3). Moreover, the liver is a central immune organ that is particularly enriched in innate immune cells and is constantly exposed to circulating nutrients and endotoxins derived from the gut microbiota (GM) that contribute to the progression and development of both MASLD and ALD^(1,4,5).

The development of culture-independent methods, such as 16S rRNA sequencing, has tremendously improved our ability to identify the different types of microorganisms associated with various disease states. Additionally, the performance of transcriptomics, metabolomics, and proteomics analysis allows the identification of its functionality in the host, promoting the elucidation of certain mechanisms, and the modulation of its effects on human pathophysiology^(1,6). Overall, there is currently insufficient

evidence that there is a specific GM signature for each liver disease. However, it is known that the composition and diversity of the GM can be influenced by several factors, such as excessive consumption of alcohol, a diet high in fat or sugar, which can lead to the development of obesity, metabolic syndrome, and liver injury^(5,7,8).

Gut dysbiosis and GM are involved in the development and progression of MASLD and ALD pathological processes⁽⁹⁾. However, whether dysbiosis plays a causal role or represents an epiphenomenon in these disease processes is incompletely elucidated and requires further investigation. The effects of host genetics as well as epigenetics, dietary modifications, and antibiotic use further complicate our understanding but pose exciting challenges and prospects for the field. Thus, considering the similarities between MASLD and ALD, the main objective of this study is to compare the composition of GM in experimental models of MASLD and ALD.

METHODS

The experimental models of MASLD and ALD that were used for the development of this study are described below (FIGURE 1 A-B).

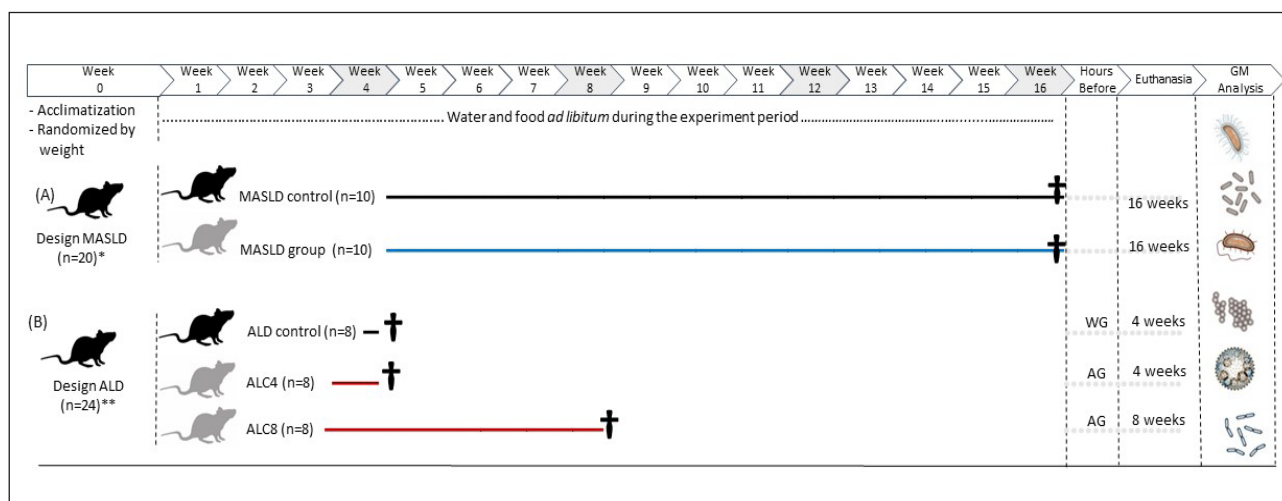


FIGURE 1. Experimental Design. **(A)** MASLD experimental model: MASLD -control group received a standard diet and water *ad libitum*; the MASLD -group received a high-fat and choline-deficient diet and water *ad libitum* during the 16-week experiment. After all the animals were euthanized. **(B)** Experimental model of ALD. The ALD-control group received a standard diet and water with 0.05% sodium saccharin *ad libitum* for four weeks. ALC4 and ALC8 groups receive a diet rich in fat from sunflower seeds without sterile husks and alcohol in a 10% ethanol solution plus 0.05% sodium saccharin. Furthermore, on the last day of the experiment, the animals received an alcoholic binge by gavage at a dose of 5g of ethanol per kilogram of the animal's weight. The experiment lasted 4 and 8 weeks, respectively. Legend: Standard diet (black line); High-fat and choline-deficient diet (blue line); High-fat diet + 10% ethanol solution; + euthanasia (red line). Abbreviations: AG: alcoholic binge by gavage (5g ethanol / kg); ALC4: alcohol group 4 weeks; ALC8: alcohol group 8 weeks; ALD: alcoholic liver disease; GM: gut microbiota; MASLD: metabolic-dysfunction associated steatotic liver disease; WG: gavage with water. *Sprague Dawley rats; **Wistar rats.

Animals and experimental model of metabolic-dysfunction associated steatotic liver disease

Twenty adults (60 days old) male *Sprague Dawley* rats weighing 280 - 350g were used. The animals were kept in groups inside two polypropylene boxes, kept in a controlled temperature environment (22±2°C) and a 12-hour light/dark cycle. All experimental procedures were approved by the Ethics Committee for the Use of Animals (No. 17-0531) in accordance with international guidelines for animal welfare and measures were taken to minimize animal pain and discomfort.

After acclimatization to the environment, the animals were randomized into two experimental groups according to their weight, as described in a previous publication⁽¹⁰⁾. A MASLD-control group (MASLD-control; n=10) that received the standard diet (Nuvilab CR-1, Quimtia S.A., Brazil) and MASLD-group (MASLD; n=10) that received high fat and choline-deficient (HFCD) diet, for steatohepatitis induction, consisting of 31.5% total fat, enriched with 54.0% trans fatty acids (Rhoster Ltda., Brazil). Both groups received water and food *ad libitum* during the experiment. All animals were euthanized after 16 weeks of the experiment. The rats were anesthetized with isoflurane and euthanized by cardiac exsanguination. The feces present in the intestine were collected aseptically and kept at -80°C until GM analysis. A portion of the liver tissue was fixed in 10% formalin for histological analysis. The experimental model is represented in FIGURE 1A.

Animals and experimental model of alcoholic liver disease

Twenty-four adult (60 days old) male Wistar rats, weighing between 260–340 g, were kept under the same conditions as previously described. All experimental procedures were approved by the Ethics Committee for the Use of Animals (No. 2018-0257) and were conducted in accordance with international guidelines for the care and use of laboratory animals.

After acclimatization to the environment, the animals were randomized into three experimental groups according to their weight, as described in a previous publication⁽¹¹⁾. An ALD-control group (ALD-control; n=8), 4-weeks alcohol group (ALC4; n=8); and 8-weeks alcohol group (ALC8; n=8). The trial period was

four and eight weeks for groups ALC4 and ALC8, respectively. During the four weeks of the experiment, the animals in the ALD-control group received a standard diet (Nuvilab CR-1, Quimtia S.A., Brazil) *ad libitum*, consisting of 4.5% lipids, 55.0% carbohydrates, 22.0% protein and 18.5% fibers and vitamins (14 J/g; information provided by the manufacturer). The addition of 0.05% sodium saccharin was added to the drinking water of these animals. Additionally, nine hours before euthanasia, these experimental groups received the gavage with water. The animals in groups ALC4 and ALC8 received *ad libitum* a high-fat diet of sunflower seeds without sterile husk and alcohol through a 10% ethanol solution (Merck PA, Germany) together with 0.05% sodium saccharin, with the objective of increasing the palatability of the alcoholic solution. Additionally, nine hours before euthanasia, these experimental groups received an alcoholic binge by gavage at a dose of 5g of ethanol per kilogram of the animal's weight. The high-fat diet of sunflower consisted of 47.3% lipids, 19.9% carbohydrates, 24.0% protein, and 8.8% fibers (25 J/g). All animals were anesthetized with isoflurane and euthanized by cardiac exsanguination. The feces present in the intestine were collected aseptically and kept at -80°C until GM analysis. Part of the liver tissue was fixed in 10% formalin for histological analysis. The experimental model is represented in FIGURE 1B.

Histopathological analysis

Samples of liver tissue fixed in formalin were included in paraffin and stained with hematoxylin & eosin (H&E) and picrosirius to identify fibrosis. Histopathological evaluation of the hepatic tissue from the experimental MASLD model was conducted according to the scoring system proposed by Liang et al, which is a highly reproducible scoring system and applicable to the experimental models in rodents⁽¹²⁾. For the experimental ALD model, histopathological evaluation was conducted using the adapted Kleiner et al. score⁽¹³⁾. Therefore, the evaluation was performed based on the degrees of severity of steatosis: 0 (occurrence in up to 5% of the tissue), 1 (occurrence in 6–33% of the tissue), 2 (occurrence in 34–66% of the tissue) and 3 (between 67 and 100% of the tissue). The evaluations of both experimental models were conducted by the same experienced patholo-

gist who was blind to the experimental groups. Fibrosis was quantified by morphometric analysis after picosirius staining. The slides were photographed using the Olympus BX51 microscope.

DNA extraction and 16S rRNA sequencing

The bacterial DNA was isolated from the fecal samples using the QIAamp fast DNA stool mini kit (Qiagen, USA), following the manufacturer's instructions. The hypervariable V4 region from the rRNA gene was amplified by PCR using the following primer pair: 515F (5'-GTGCCAGCMGCCGCGGTAA-3') and 806R (5'-GGACTACHVGGGTWTCTAAT-3'). To pool different samples in the same reaction, we used the primer-fusion method and each sample had a distinct barcode attached on the corresponding PCR product. The purified products were subjected to emulsion PCR using Ion PGM™ Hi-Q™ view OT2 kit (Thermo Fisher Scientific, USA). After, the resulting enriched beads were sequenced in a next-generation sequencing machine using Ion PGM™ Hi-Q™ view sequencing kit (Thermo Fisher Scientific, USA).

Bioinformatics analyses

The sequence data exported from the Ion PGM™ System was processed using a custom pipeline in Mothur v.1.41.1⁽¹⁴⁾. Initially, sequences were depleted of barcodes and primers (where no mismatch was allowed) and then a quality filter was applied to eliminate low quality reads. Quality control was conducted by trimming the low-quality reads, those with incorrect length, those containing an ambiguous base, or containing homopolymers longer than 8bp. All potentially chimeric sequences were identified and removed using VSEARCH⁽¹⁵⁾.

After this initial quality, filtering and trimming steps, the remaining sequences were clustered into operational taxonomic units (OTUs) based on a 99% identity level and were classified against the SILVA v132 reference database at 97% similarity⁽¹⁶⁾. Sequences that could not be classified (i.e., "unknown" sequences), as well as sequences identified as eukaryotes, mitochondria, and chloroplasts were removed prior to further analysis. The resulting OTU table was rarefied to the smallest library size. Subsequent analyses of the sequence dataset were performed in R v. 4.0.0 (using vegan, phyloseq, ggplot2, and MicrobiomeAnalystR packages).

Microbial community and statistical analysis

Alpha diversity was assessed using the number of observed taxa as well as ACE and Shannon index. For the overall comparison of significant differences among bacterial communities (i.e., beta diversity), principal coordinates analysis (PCoA) was performed. A matrix using the Bray–Curtis dissimilarity metric was calculated for each pair of samples. To achieve statistical confidence for the sample grouping observed by PCoA, the ANOSIM multivariate test was performed on the distance matrix. To compare additional differences among the microbial communities, clustering methods based on Bray–Curtis dissimilarity were performed. The results of hierarchical clustering were visualized using dendrograms. Venn dendrogram was generated using InteractiVenn.

To identify differentially abundant taxa at the phylum, family, and genus level, the linear discriminant effect size (LEfSe) method was performed. The algorithm performs a nonparametric factorial Kruskal–Wallis sum rank test and linear discriminant analysis (LDA) to determine statistically significant different features among taxa and estimates the effect size of the difference. Differences were considered significant for a logarithmic LDA score threshold of ± 1.5 and a $P < 0.05$.

RESULTS

General characteristics of experimental models

Animals in MASLD model exhibited marked deposition of body and hepatic fat, activation of microRNAs, receptors, mediators, and inflammatory cytokines, along with an increased risk of developing cardiovascular diseases. On the other hand, animals in ALD model presented, significant alterations in body composition were demonstrated, suggesting worsening nutritional status, biochemical changes, and hepatic fat deposition in the ALC4 and ALC8 groups^(7,10,11). Regarding the histopathological evaluation of the liver in the experimental MASLD model, no hepatic abnormalities were reported in the liver tissue of the MASLD-control group (FIGURE 2A), whereas the animals in the MASLD-group had predominantly microvesicular steatosis along with macrovesicular steatosis of moderate intensity, with inflammatory activity and a mild degree of fibrosis

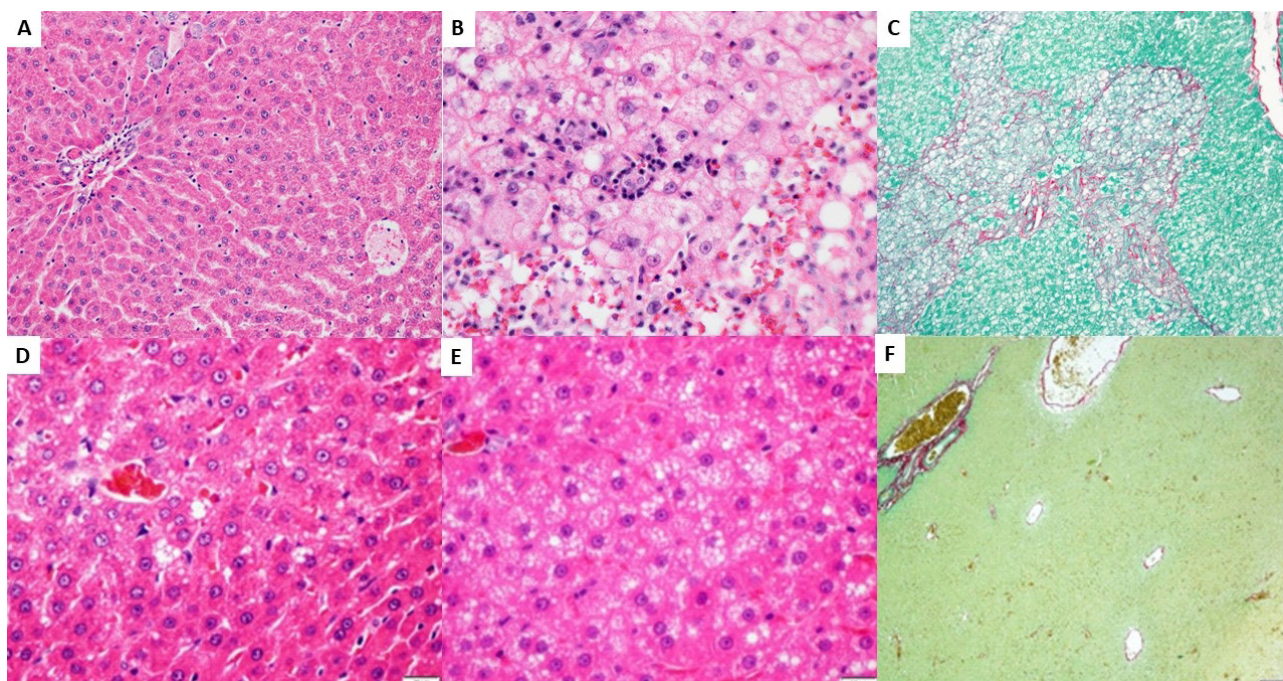


FIGURE 2. Liver histological evaluation. Images depict the MASLD-control group (A) at 20X magnification with H&E staining; the MASLD-group (B) at 40X magnification with H&E staining; picrosirius staining at 10X magnification in the MASLD-group (C). In the ALD model, hepatic histology is shown with H&E staining in the ALC4 (D) and ALC8 (E) groups, both at 400X magnification. Additionally, hepatic histology staining with picrosirius is shown at 40X magnification in group (F) ALC8, with no detectable collagen deposition. Abbreviations: ALC4: alcohol group 4 weeks; ALC8: alcohol group 8 weeks; H&E: hematoxylin & eosin; MASLD: metabolic-dysfunction associated steatotic liver disease.

(FIGURE 2B-C). In the experimental model of ALD, there were no abnormalities in the liver tissue of animals in the CONT group, while animals in the ALC4 (FIGURE 2D) and ALC8 (FIGURE 2E) groups showed micro and macrovesicular steatosis. No deposition of collagen fibers in the hepatic tissue was observed in any experimental group through picrosirius staining (FIGURE 2F).

Gut microbiota diversity and composition

Regarding alpha diversity, the experimental model of MASLD showed a significant decrease in the ACE index ($P < 0.001$; FIGURE 3A) and Chao1 index ($P = 0.049$; FIGURE 3B) in relation to the experimental model of ALD. Animals in the MASLD-group and those submitted to excessive alcohol consumption for 8 weeks (ALC8) showed a significant decrease in the Shannon index ($P \leq 0.021$; FIGURE 3C), in relation to the other groups. Animals from the ALC4 group and their respective control group (ALD-control) showed a significant increase in observed taxa ($P = 0.001$; FIGURE 3D), in relation to the others.

To explore the global differences in gut bacterial

communities between groups, a PCoA analysis (FIGURE 4A) and dendrogram clustering (FIGURE 4B) of sample was performed on OTUs-based Bray–Curtis distances. Through this evaluation, we observed that the structural pattern of the GM of the experimental model of MASLD is clearly distinct from the experimental model of ALD (ANOSIM, $P < 0.001$).

Gut microbiota composition

In the evaluation of the Venn diagram (FIGURE 5), we observed that the MASLD-group and the animals subjected to excessive alcohol consumption for 4 and 8 weeks (ALC4 and ALC8, respectively) shared a total of 26 taxa at the genus level. The ALC4 and ALC8 groups had 14 and 6 exclusive genera, respectively. Additionally, these groups subjected to excessive alcohol consumption shared 17 unique genera of bacteria. We report six genera exclusive to animals with MASLD, in addition six genera of bacteria were shared with the ALC4 group and four with the ALC8 group. Information on shared and unique genres among the experimental groups is described in SUPPLEMENTAL TABLE-1.

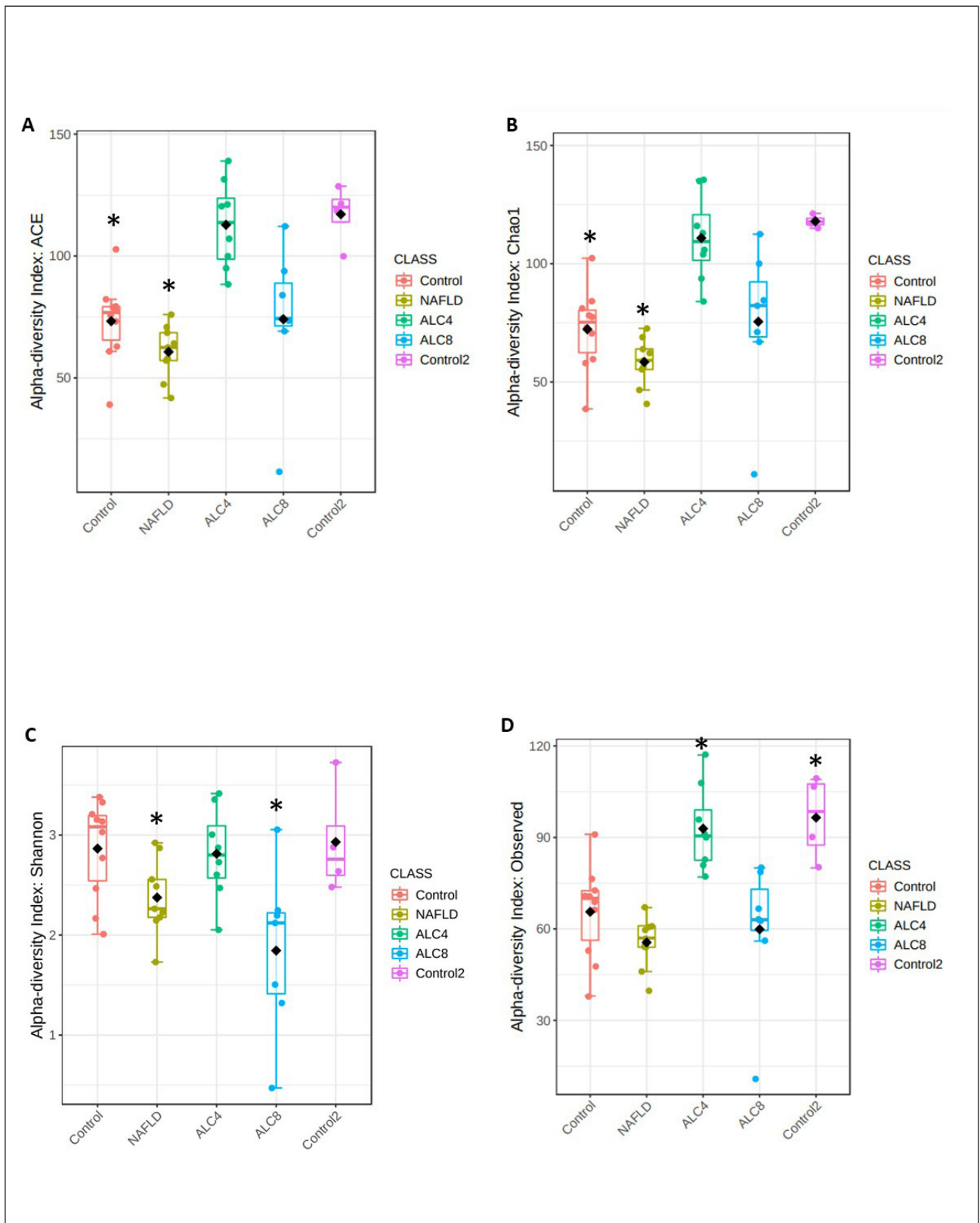


FIGURE 3. Alpha diversity analysis according to different metrics. (A) ACE, (B) Shannon, (C) Observed and, (D) Chao1 richness estimator. Statistical confidence was accessed using the multivariate Kruskal-Wallis test. Asterisks indicate the P -value < 0.05 . The acronym MASLD represents the NAFLD (non-alcoholic fatty liver disease) information in the image. Abbreviations: ALC4: alcohol group 4 weeks; ALC8: alcohol group 8 weeks; NAFLD: non-alcoholic fatty liver disease.

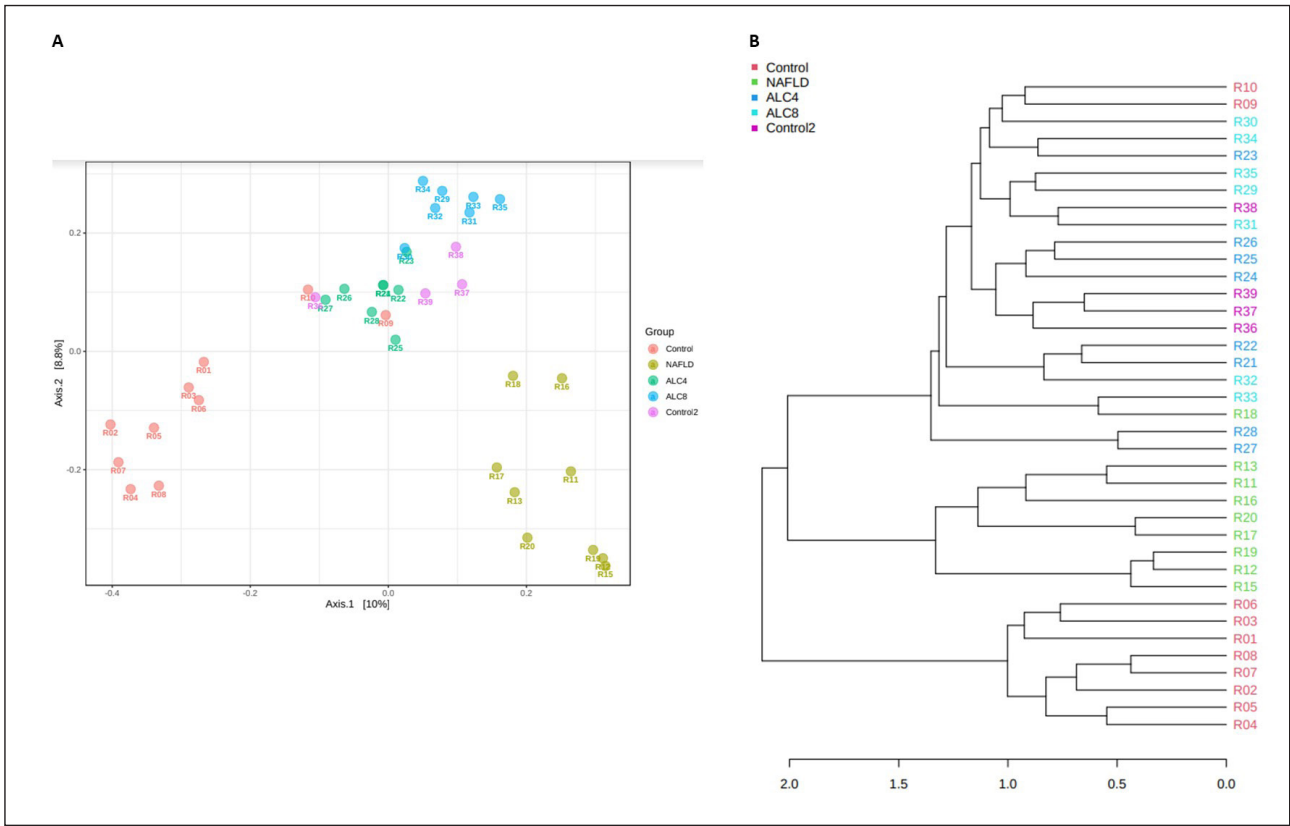


FIGURE 4. (A) Principal coordinate analysis (PCoA) of the bacterial community structures of all groups based on Bray-Curtis distance metric and (B) Hierarchical clustering dendrogram based on the Bray-Curtis dissimilarity index. Samples were colored according to the experimental group. Statistical confidence for the sample grouping was accessed using analysis of similarities (ANOSIM). The acronym MASLD represents the NAFLD (non-alcoholic fatty liver disease) information in the image. Abbreviations: ALC4: alcohol group 4 weeks; ALC8: alcohol group 8 weeks; NAFLD: non-alcoholic fatty liver disease.

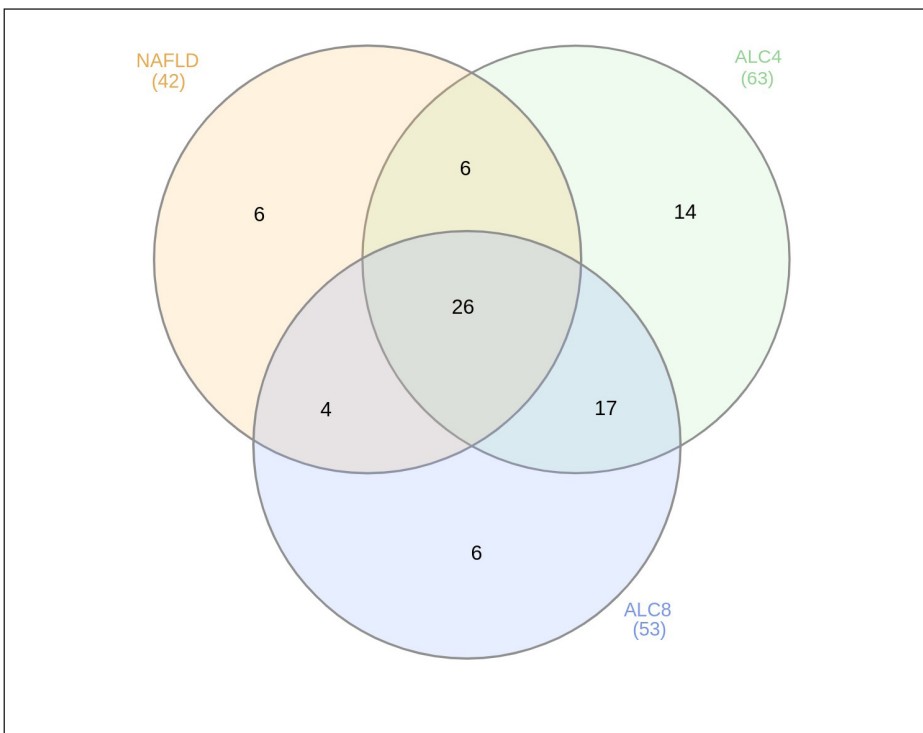


FIGURE 5. Venn diagram showing unique and shared taxa at the genus level among the NAFLD, ALC4, and ALC8 experimental groups. Venn diagram showing unique and shared taxa at the genus level among the NAFLD, ALC4, and ALC8 experimental groups. The acronym MASLD represents the NAFLD (non-alcoholic fatty liver disease) information in the image. Abbreviations: ALC4: alcohol group 4 weeks; ALC8: alcohol group 8 weeks; NAFLD: non-alcoholic fatty liver disease.

SUPPLEMENTARY TABLE 1. Description of bacterial genera in the MASLD, ALC4 and ALC8 experimental groups.

MASLD	ALC4	ALC8
Bacteroides	Lactobacillaceae_unclassified	Bacteroides
Romboutsia	Muribaculaceae_ge	Clostridia_UCG_014_ge
Muribaculaceae_ge	Lachnospiraceae_NK4A136_group	Muribaculaceae_ge
uncultured	Bacteroides	Lachnospiraceae_unclassified
Oscillospirales_ge	Muribaculaceae_unclassified	Gastranaerophilales_ge
Lachnospiraceae_unclassified	Lachnospiraceae_unclassified	Akkermansia
UBA1819	Romboutsia	Oscillospiraceae_unclassified
Bacteroidales_unclassified	Turicibacter	Ruminococcus
UCG_005	Bacteroidales_unclassified	Parasutterella
Alistipes	Clostridia_UCG_014_ge	Tannerellaceae_unclassified
Sutterella	Monoglobus	Clostridia_unclassified
Oscillospiraceae_unclassified	Anaeroplasm	Muribaculaceae_unclassified
UCG_009	uncultured	Monoglobus
Clostridiaceae_unclassified	Clostridia_unclassified	Limosilactobacillus
Turicibacter	Oscillospirales_ge	UBA1819
Limosilactobacillus	Oscillospiraceae_unclassified	Bilophila
NK4A214_group	Limosilactobacillus	Parabacteroides
Muribaculaceae_unclassified	Ruminococcaceae_unclassified	Sellimonas
Intestinimonas	Lactobacillus	Alistipes
Blautia	Lachnospiraceae_NC2004_group	Lactobacillaceae_unclassified
Lactococcus	Ligilactobacillus	Oscillospirales_ge
Christensenellaceae_R_7_group	Streptococcus	Clostridia_vadinBB60_group_ge
Enterobacteriaceae_unclassified	Ruminococcus	Rhodospirillales_unclassified
Sellimonas	Alistipes	Intestinimonas
Akkermansia	Prevotellaceae_unclassified	Sutterella
Frisingicoccus	RF39_ge	Oscillospirales_unclassified
Parasutterella	Gastranaerophilales_ge	Ruminococcaceae_unclassified
Tannerellaceae_unclassified	Clostridiaceae_unclassified	UCG_008
Oscillibacter	Lachnospiraceae_UCG_001	Lachnospiraceae_NK4A136_group
Erysipelatoclostridiaceae_ge	Ruminococcaceae_ge	Marvinbryantia
Colidextribacter	UCG_003	Colidextribacter
Marvinbryantia	Christensenellaceae_R_7_group	uncultured_ge
Ruminococcaceae_unclassified	Muribaculum	Lachnospira
Parabacteroides	Rikenellaceae_RC9_gut_group	Ligilactobacillus
Lactobacillus	Parasutterella	Anaeroplasm
Gastranaerophilales_ge	Oscillibacter	uncultured
Firmicutes_unclassified	Roseburia	Romboutsia
Anaerovoracaceae_unclassified	Helicobacter	Incertae_Sedis
Muribaculum	Clostridia_vadinBB60_group_ge	Blautia
Clostridia_UCG_014_ge	Rikenellaceae_unclassified	Helicobacter
Lactobacillaceae_unclassified	Marvinbryantia	Paludicola
Tannerellaceae_ge	Mucispirillum	Streptococcus
	Anaerostipes	Anaerostipes
	Lachnospiraceae_NK4B4_group	Lachnospiraceae_ND3007_group
	Akkermansia	Frisingicoccus
	UCG_005	Turicibacter
	Lachnospiraceae_UCG_006	Mucispirillum
	Bifidobacterium	Peptococcus
	Colidextribacter	Erysipelatoclostridiaceae_unclassified
	Lachnospiraceae_ND3007_group	Bacteroidales_unclassified
	UCG_010_ge	Bifidobacterium
	Incertae_Sedis	Anaerovoracaceae_unclassified
	Sutterella	Enterobacteriaceae_unclassified
	Shuttleworthia	
	Frisingicoccus	
	Intestinimonas	
	Parabacteroides	
	Anaerovoracaceae_unclassified	
	Tannerellaceae_unclassified	
	uncultured_ge	
	Peptococcus	
	Paludicola	
	Butyricocccaceae_unclassified	

ALC4: alcohol group 4 weeks; ALC8: alcohol group 8 weeks; MASLD: metabolic-dysfunction associated steatotic liver disease.

Taxonomy-based analysis of bacterial communities identified 947 bacterial taxa (OTUs), belonging to 83 genera, 39 families, and 9 phyla. *Bacteroidetes* (55.7%), *Firmicutes* (40.6%), and *Proteobacteria* (1.4%) were the most prevalent phyla in all samples, additionally, these three phyla were also differentially abundant among the experimental groups (FIGURE 6). The ALC8 group presented a greater abundance of the phyla *Cyanobacteria* (5.3%) and *Verrucomicrobiota* (3.2%) in relation to the other groups. *Proteobacteria* were more abundant in the ALC4 and ALD-control groups (3.2% in both groups) compared to the others. Other phyla had less than 1% abundance each.

The most abundant families were *Bacteroidaceae* (25.3%), *Muribaculaceae* (24.5%), *Lachnospiraceae* (14.1%), and *Lactobacillaceae* (6.1%). These four families represented 70.0% of all observed taxa. Differences in the abundance of bacterial families were observed between the experimental groups of the MASLD and ALD models (FIGURE 7). In the experimental model of MASLD, we observed that the families of bacteria prevalent in the MASLD-control group were less prevalent (or absent) compared to the MASLD-group, while the inverse was also reported. In the experimental model of alcohol abuse, we reported a greater abundance of *Lactobacillaceae* (26.7%) and *Lachnospiraceae* (17.0%) in the ALC4

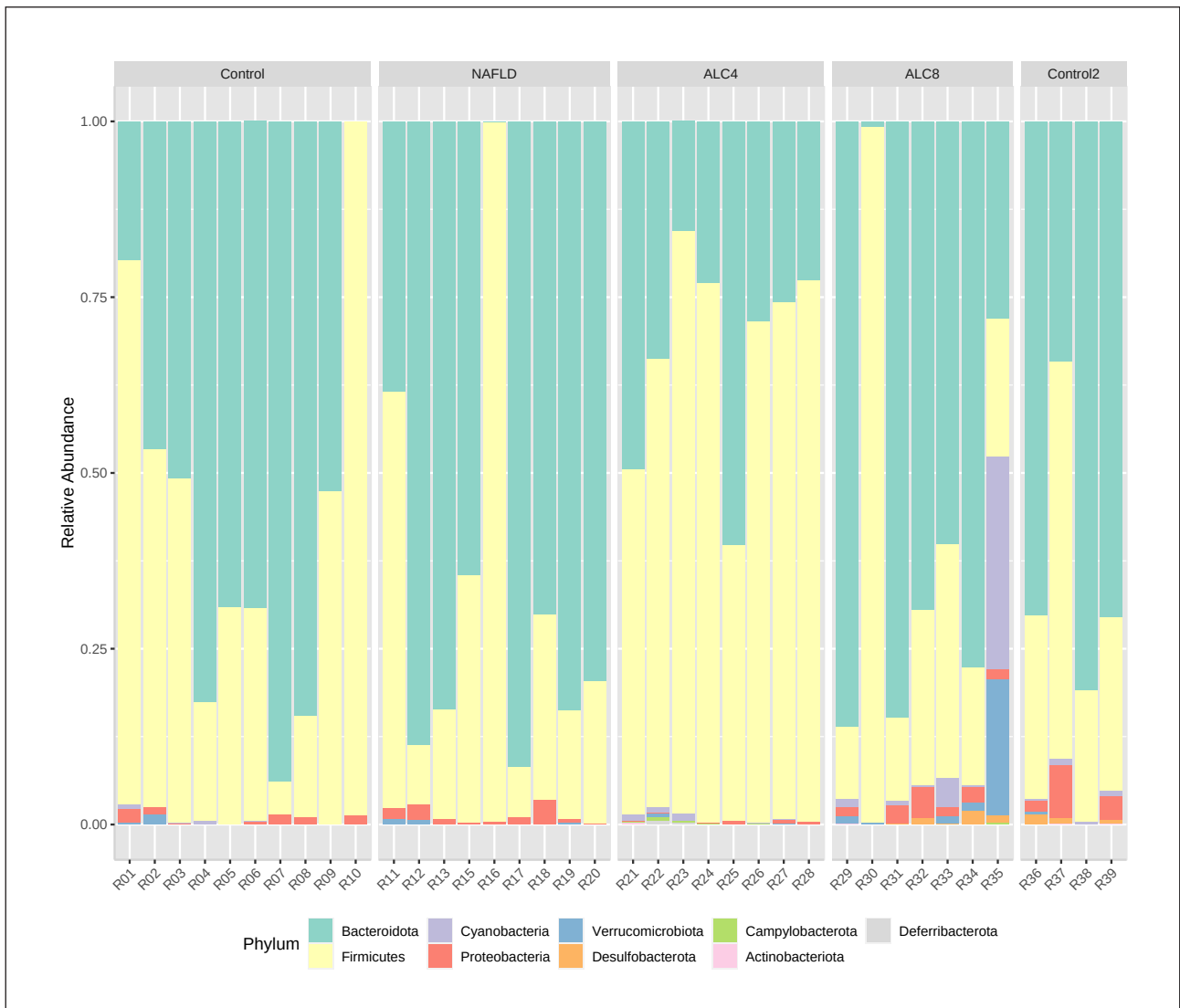


FIGURE 6. Composition of intestinal microbiota at the phylum level. The acronym MASLD represents the non-alcoholic fatty liver disease (NAFLD) information in the image. Abbreviations: ALC4: alcohol group 4 weeks; ALC8: alcohol group 8 weeks; NAFLD: non-alcoholic fatty liver disease.

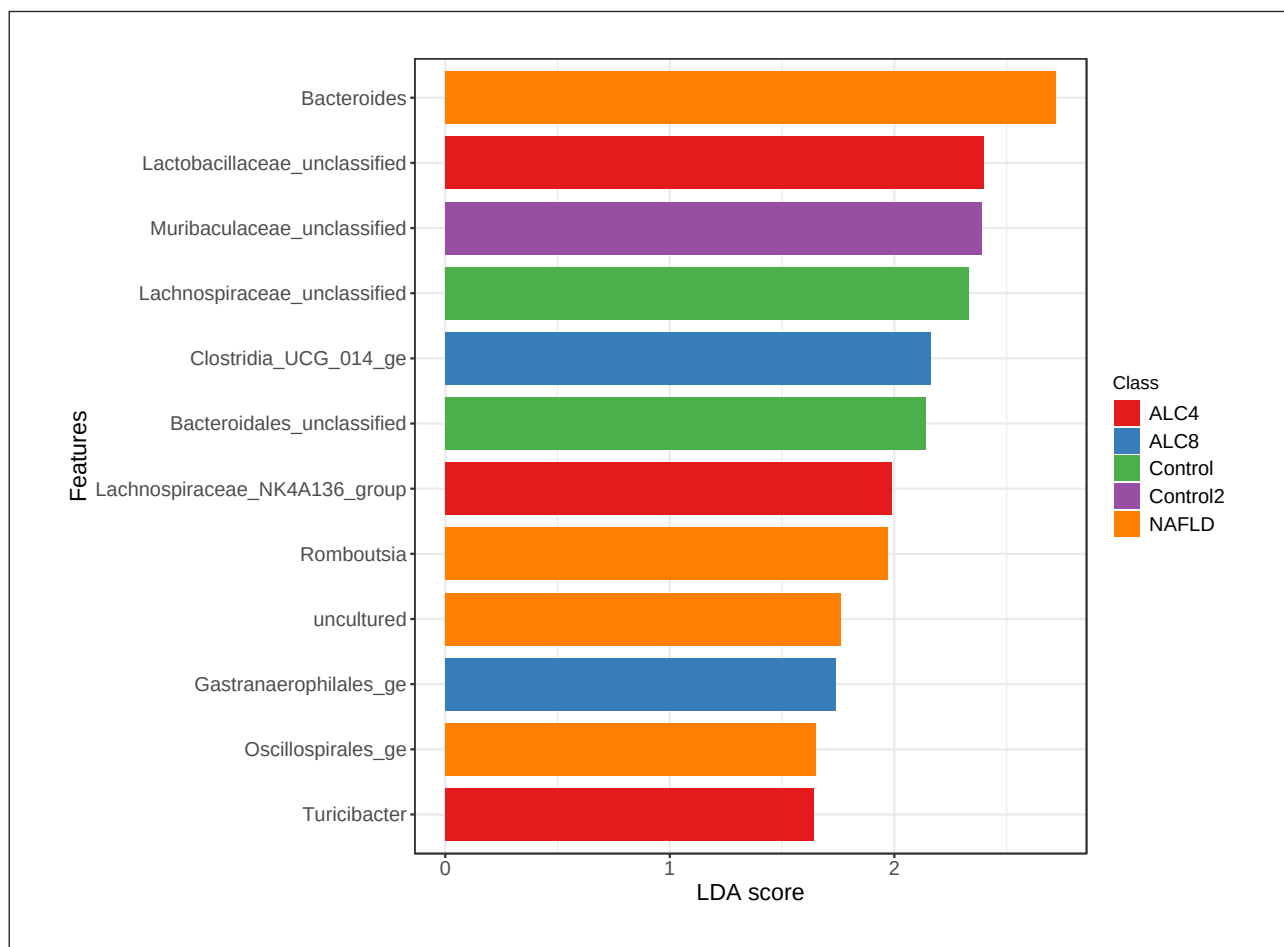


FIGURE 7. Composition of intestinal microbiota at the family level. The acronym MASLD represents the non-alcoholic fatty liver disease (NAFLD) information in the image. Abbreviations: ALC4: alcohol group 4 weeks; ALC8: alcohol group 8 weeks; NAFLD: non-alcoholic fatty liver disease.

group, additionally; a greater abundance of *Bacteroidaceae* (44.3%) and *Clostridia_UCG* (14.0%) was reported in the group ALC8. The abundance of the *Muribaculaceae* family of bacteria was 41.2% in the ALD-control group, 20.6% in the ALC4 group, and 11.78% in the ALC8 group.

In the analysis of the differential abundance, we identified four genera associated with the MASLD-group and two associated with its MASLD-control group. This evaluation reported a greater abundance of *Bacteroides*. Differential abundance analysis identified *Lactobacillaceae_unclassified*, *Lachnospiraceae_NK4A136_group*, and *Turicibacter* associated with the ALC4 group and the *Clostridia_UCG_014_ge* and *Gastranaerophilales_ge* genera related to the ALC8 group. In the experimental model of ALD, the ALD-control group presented a greater abundance of *Muribaculaceae_unclassified* (FIGURE 8).

DISCUSSION

Dysregulations of GM composition, microbial metabolism, and gut barrier function play a key role in the development and progression of MASLD and ALD. Both diseases are global health issues, and their incidence is increasing^(9,17). They present similar histopathological findings and, due to interindividual and interethnic differences, the involvement of genetic and epigenetic factors in both pathogenesis is suggested^(18,19). Currently, metabolic-dysfunction associated steatohepatitis (MASH) secondary cirrhosis is the second most common indication for liver transplantation, with ALD being the leading cause in adults in the United States^(17,20). Changes in the composition of the GM may explain the progression of MASLD and ALD, as bioactive metabolites are formed from endogenous (bile acids) and exogenous

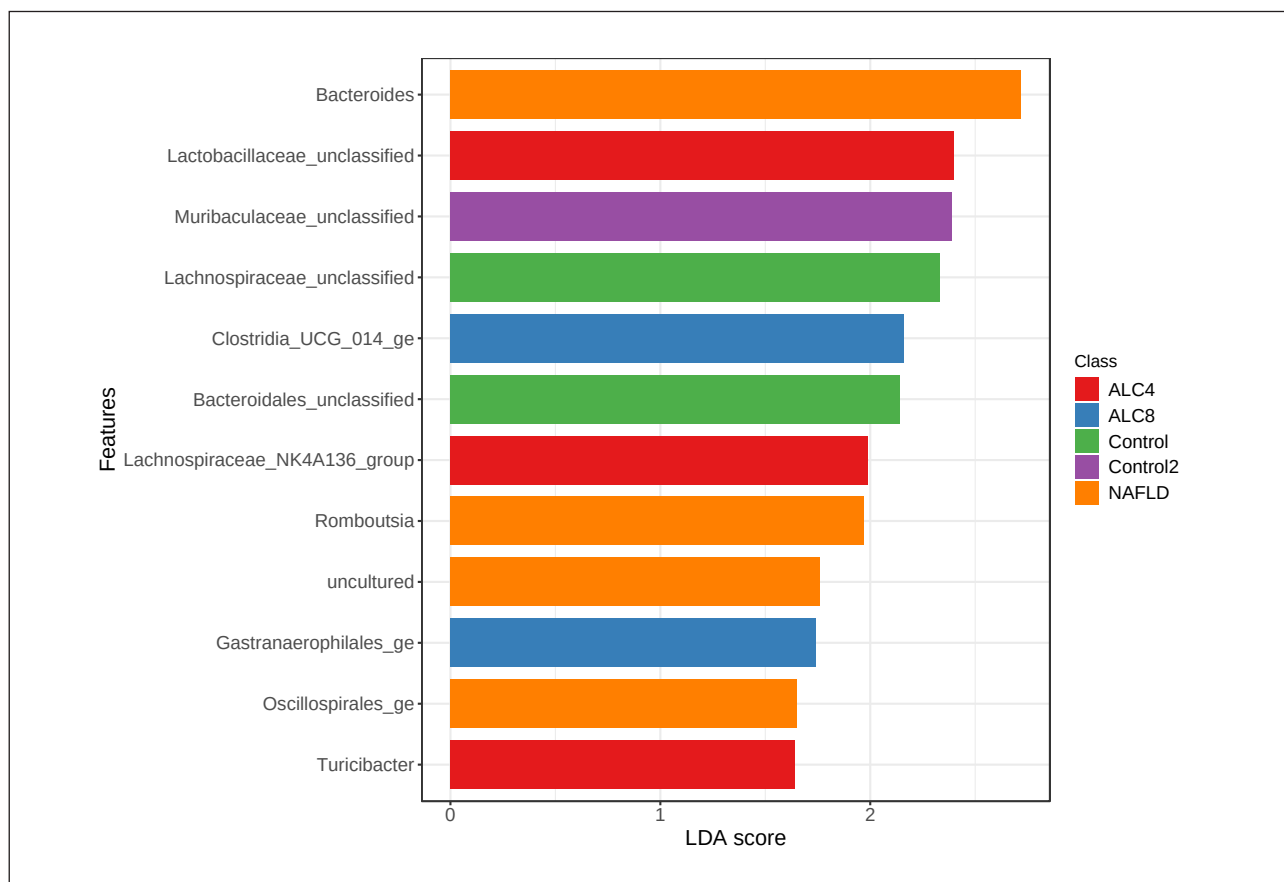


FIGURE 8. Differential abundance by linear discriminant analysis. The acronym MASLD represents the non-alcoholic fatty liver disease (NAFLD) information in the image. Abbreviations: ALC4: alcohol group 4 weeks; ALC8: alcohol group 8 weeks; NAFLD: non-alcoholic fatty liver disease.

(diet and environment) substrates and these metabolites are translocated to the liver⁽¹⁷⁾. In this study, we demonstrated that the structural pattern of the GM differs significantly between MASLD and ALD experimental models. *Bacteroidetes*, *Firmicutes*, and *Proteobacteria* were the most abundant phyla in the experimental groups studied, but differences in the abundance of bacterial families were noted. In the experimental model of MASLD, the most abundant bacterial families were less abundant (or absent) in the control group than in the MASLD-group, and the opposite was also observed. In the experimental model ALD, the ALC4 group had higher abundance of *Lactobacillaceae* and *Lachnospiraceae*, whereas the ALC8 group had increased abundance of *Bacteroidaceae* and *Clostridia_UCG*. In addition, differential abundance analysis revealed different patterns of bacterial family associations between experimental groups.

Several studies have reported the composition

of the GM in preclinical models and in patients with MASLD, but the observed results are inconsistent and contradictory^(7,9,17,21). In each stage of MASLD, there is a specific signature of the GM, but the results are still incomplete⁽²²⁻²⁵⁾. In our study, we found that the most abundant bacterial phyla are *Bacteroidetes*, *Firmicutes*, and *Proteobacteria*, but that other phyla such as *Verrucomicrobia*, *Actinobacteria*, and *Cyanobacteria* are also associated with the pathogenesis of liver injury, results that corroborate the data reported^(21,24,25). Differential abundance analysis revealed an increase in the abundance of the genera *Bacteroides*, *Romboutsia*, and *Oscillospirales_ge* in the MASLD-group. The greater abundance of the genus *Bacteroides* and the phylum *Bacteroidetes* in the MASLD-group and the decrease in *Firmicutes* observed in this study corroborates previous studies^(25,26). The increase in the abundance of the genus *Bacteroides* is related to the pathogenesis of MASLD and in particular to

MASH, as it shows strong positive correlations with the metabolites deoxycholic acid, D-pinitol, choline, raffinose, and stachyose⁽²⁵⁾. The latter two metabolites include glucose and fructose, both sugars that have been associated with increased inflammation and liver fibrosis in patients with MASLD in excess^(25,27). In addition, the increase in *Bacteroides* promotes a decrease in fecal short-chain fatty acids and amino acids, which are products of bacterial fermentation of carbohydrates associated with various beneficial effects on the organism and may be detrimental to MASLD^(25,26,28). *Bacteroides* are also responsible for the endogenous production of ethanol in MASLD, and when produced in excess, it can cause fluctuations in redox potential and increased inflammatory responses^(17,23). In this study, the bacterial genera *Romboutsia* and *Oscillospirales_ge* were more abundant in the MASLD-group than in the other groups. The data confirm previous findings reported in the literature, although their physiological effects on MASLD have not been fully elucidated⁽²⁹⁻³²⁾. The increased incidence of *Romboutsia* is associated with obesity and gut inflammation and shows a strong positive correlation with serum concentrations of low-density lipoprotein (LDL) cholesterol, a risk factor for the development of cardiovascular disease^(29,30). The increased cardiovascular risk of this MASLD experimental model was previously demonstrated by our research group, supporting the increased abundance of the *Romboutsia* genus⁽⁷⁾.

Experimental models for ALD are difficult to establish as rodents have aversion to alcohol^(11,33). Other described models are expensive and difficult to reproduce because they either require special diets, infusion pumps or invasive procedures^(34,35). However, the development of experimental models to elucidate the pathophysiological mechanisms of ALD and to evaluate potential therapeutic strategies is essential. The model developed by our group is capable of triggering ALD at an early stage with histopathological and biochemical changes in liver function that correspond to the phenotype of the disease in human⁽¹¹⁾. The severity of alcohol-induced liver injury might be related to a specific signature of GM composition. In our study, animals exposed to alcohol abuse for eight weeks had high abundance of *Cyanobacteria* and *Verrucomicrobiota* phyla.

Cyanobacteria induce the production of liver toxins such as microcystins, which promote the formation of reactive oxygen species and inflammation⁽³⁶⁾. The damage caused depends on the level and duration of exposure to microcystins, which may explain the increase in this phylum, especially in animals from the ALC8 group compared to the ALC4 group⁽³⁶⁾. An experimental model of continuous intragastric alcohol feeding showed an increase in the relative abundance of the *Verrucomicrobiota* phylum, a finding that supports our findings⁽³⁷⁾. In this study, an increase in the relative abundance of the genus *Turicibacter* was demonstrated, especially in the group exposed to alcohol abuse for four weeks. As previously reported, this bacterial species is associated with an increase in pro-inflammatory response and is also positively correlated with the severity of ethanol-induced liver injury^(38,39). In preclinical models and in patients with ALD, we found no reports of *Lactobacillaceae*, *Lachnospiraceae*, *Clostridia_UCG*, and *Gastranaerophilales_ge*, making it difficult to discuss the results. This can be attributed to the different molecular techniques used to evaluate the composition of the microbiota, which is a limitation⁽²⁴⁾. In addition, several studies evaluating the composition of the GM describe only the taxonomy of some bacterial species. In addition, we emphasize the need for further studies in which proteomics and metabolomics assessments are performed to elucidate the impact of microbial function on liver lesions.

In conclusion, we report that the structural pattern of the GM in MASLD is significantly different from ALD. To our knowledge, this is the first report that provides a comparative assessment of the composition of the GM in preclinical models of MASLD and ALD. Changes in GM composition are associated with the development and progression of liver lesions, but more studies combining assessments of bacterial gene expression and bioactive metabolites are needed^(17,40). The goal is to provide new insights for future modulation of the GM and supplementation of bacterial metabolites for therapeutic benefit.

Authors' contribution

Longo L, Perlin CM, and Álvares-da-Silva MR performed the conceptualization, methodology, formal analysis, investigation, data curation, writing of the

original draft, writing-review, and editing; Thoen RU, and Uribe-Cruz C performed the conceptualization, methodology, and formal analysis. Perlin CM and Longo L contributed equally to the writing of this article. All authors have read and agreed to the published version of the manuscript.

Orcid

Cássio Marques Perlin: 0000-0003-2651-7588.

Larisse Longo: 0000-0002-4453-7227.

Rutiane Ullmann Thoen: 0000-0001-8174-0366.

Carolina Uribe-Cruz: 0000-0002-0526-3067.

Mário Reis Álvares-da-Silva: 0000-0002-5001-246X.

Perlin CM, Longo L, Thoen RU, Uribe-Cruz C, Álvares-da-Silva MR. Comparação da microbiota intestinal em modelos animais de doença hepática esteatótica alcoólica e metabólica. *Arq gastroenterol.* 2024;61:e23100.

RESUMO – Contexto – A doença hepática alcoólica (DHA) e a doença hepática esteatótica associada à disfunção metabólica (MASLD) são comuns, e a microbiota intestinal (MI) está envolvida em ambas. Aqui, comparamos a composição da MI em modelos animais de MASLD e DHA para avaliar se existem padrões específicos para cada doença. **Métodos** – Modelo de MASLD – ratos machos adultos da linhagem *Sprague Dawley*, randomizados em dois grupos: MASLD-controle (n=10) alimentados com uma dieta padrão; grupo MASLD (n=10) alimentados com uma dieta rica em gordura e deficiente em colina por 16 semanas. Modelo de DHA – ratos machos adultos da linhagem Wistar randomizados: DHA-controle (n=8) alimentados com uma dieta padrão e água+0,05% de sacarina; grupos DHA alimentados com semente de girassol e 10% de etanol+0,05% de sacarina por 4 ou 8 semanas (DHA4, n=8; DHA8, n=8). DHA 4/8 no último dia receberam binge alcoólico (5 g/kg de etanol). Posteriormente, os animais foram sacrificados, e as fezes foram coletadas para análise da MI. **Resultados** – Ambos os modelos experimentais induziram características histopatológicas típicas das doenças. A diversidade alfa foi menor na MASLD em comparação com a DHA ($P<0,001$), e o padrão estrutural foi diferente entre elas ($P<0,001$). *Bacteroidetes* (55,7%), *Firmicutes* (40,6%) e *Proteobactérias* (1,4%) foram os filos mais prevalentes em todas as amostras, embora com abundâncias diferenciadas entre os grupos. DHA8 teve uma maior abundância dos filos *Cyanobacteria* (5,3%) e *Verrucomicrobiota* (3,2%) em relação aos outros. A análise de abundância diferencial identificou *Lactobacillaceae_unclassified*, *Lachnospiraceae_NK4A136* e *Turicibacter* associados ao grupo DHA4, e os gêneros *Clostridia_UCG_014_ge* e *Gastranaerophilales_ge* associados ao DHA8. **Conclusão** – Neste estudo, demonstramos que o padrão estrutural da MI difere significativamente entre os modelos de MASLD e DHA. Estudos são necessários para caracterizar a microbiota e os metabólitos ativos em ambas as condições clínicas, a fim de encontrar novas estratégias terapêuticas.

Palavras-chave – Modelo animal; doença hepática alcoólica; microbiota intestinal; doença hepática esteatótica associada à disfunção metabólica; doença hepática.

REFERENCES

- Huang W, Kong D. The intestinal microbiota as a therapeutic target in the treatment of NAFLD and ALD. *Biomed Pharmacother.* 2021;135:111235.
- Rinella ME, Lazarus JV, Ratzliff V, Francque SM, Sanyal AJ, Kanwal F, et al. A multisociety Delphi consensus statement on new fatty liver disease nomenclature. *J Hepatol.* 2023;79:1542-56. doi: 10.1016/j.jhep.2023.06.003.
- Wang H, Mehal W, Nagy LE, Rotman Y. Immunological mechanisms and therapeutic targets of fatty liver diseases. *Cell Mol Immunol.* 2021;18:73-91.
- Wang R, Tang R, Li B, Ma X, Schnabl B, Tilg H. Gut microbiome, liver immunology, and liver diseases. *Cell Mol Immunol.* 2021;18:4-17.
- Bakhshimoghaddam F, Alizadeh M. Contribution of gut microbiota to nonalcoholic fatty liver disease: Pathways of mechanisms. *Clin Nutr ESPEN.* 2021;44:61-8.
- Albhaisi SAM, Bajaj JS, Sanyal AJ. Role of gut microbiota in liver disease. *Am J Physiol Gastrointest Liver Physiol.* 2020;318:G84-G98.
- Longo L, Rampelotto PH, Filippi-Chiela E, de Souza VEG, Salvati F, Cerski CT, et al. Gut dysbiosis and systemic inflammation promote cardiomyocyte abnormalities in an experimental model of steatohepatitis. *World J Hepatol.* 2021;13:2052-70.
- Milosevic I, Vujovic A, Barac A, Djelic M, Korac M, Radovanovic Spurnic A, et al. Gut-Liver Axis, Gut Microbiota, and Its Modulation in the Management of Liver Diseases: A Review of the Literature. *Int J Mol Sci.* 2019;20:395.
- Park JW, Kim SE, Lee NY, Kim JH, Jung JH, Jang MK, et al. Role of Microbiota-Derived Metabolites in Alcoholic and Non-Alcoholic Fatty Liver Diseases. *Int J Mol Sci.* 2021;23:426.
- Longo L, Tonin Ferrari J, Rampelotto PH, Hirata Dellavia G, Pasqualotto A, P Oliveira C, et al. Gut Dysbiosis and Increased Intestinal Permeability Drive microRNAs, NLRP-3 Inflammasome and Liver Fibrosis in a Nutritional Model of Non-Alcoholic Steatohepatitis in Adult Male Sprague Dawley Rats. *Clin Exp Gastroenterol.* 2020;13:351-68.
- Thoen RU, Longo L, Leonhardt LC, Pereira MHM, Rampelotto PH, Cerski CTS, et al. Alcoholic liver disease and intestinal microbiota in an experimental model: Biochemical, inflammatory, and histologic parameters. *Nutrition.* 2022;106:111888.
- Liang W, Menke AL, Driessen A, Koek GH, Lindeman JH, Stoop R, et al. Establishment of a general NAFLD scoring system for rodent models and comparison to human liver pathology. *PLoS One.* 2014;9:e115922.
- Kleiner DE, Brunt EM, Van Natta M, Behling C, Contos MJ, Cummings OW, et al. Design and validation of a histological scoring system for nonalcoholic fatty liver disease. *Hepatology.* 2005;41:1313-21.
- Schloss PD, Westcott SL, Ryabin T, Hall JR, Hartmann M, Hollister EB, et al. Introducing mothur: open-source, platform-independent, community-supported software for describing and comparing microbial communities. *Appl Environ Microbiol.* 2009;75:7537-41.
- Rognes T, Flouri T, Nichols B, Quince C, Mahé F. VSEARCH: a versatile open source tool for metagenomics. *PeerJ.* 2016;4:e2584.
- Quast C, Pruesse E, Yilmaz P, Gerken J, Schweer T, Yarza P, et al. The SILVA ribosomal RNA gene database project: improved data processing and web-based tools. *Nucleic Acids Res.* 2013;41(Database issue):D590-6.

17. Lang S, Schnabl B. Microbiota and Fatty Liver Disease—the Known, the Unknown, and the Future. *Cell Host Microbe*. 2020;28:233-44.
18. Idalsoaga F, Kulkarni AV, Mousa OY, Arrese M, Arab JP. Non-alcoholic Fatty Liver Disease and Alcohol-Related Liver Disease: Two Intertwined Entities. *Front Med (Lausanne)*. 2020;7:448.
19. Yamamoto K, Kogiso T, Taniai M, Hashimoto E, Tokushige K. Differences in the genetic backgrounds of patients with alcoholic liver disease and non-alcoholic fatty liver disease. *JGH Open*. 2019;3:17-24.
20. Estes C, Razavi H, Loomba R, Younossi Z, Sanyal AJ. Modeling the epidemic of nonalcoholic fatty liver disease demonstrates an exponential increase in burden of disease. *Hepatology*. 2018;67:123-33.
21. Fukui H. Gut Microbiota and Host Reaction in Liver Diseases. *Microorganisms*. 2015;3:759-91.
22. Bajaj JS, Idilman R, Mabudian L, Hood M, Fagan A, Turan D, et al. Diet affects gut microbiota and modulates hospitalization risk differentially in an international cirrhosis cohort. *Hepatology*. 2018;68:234-47.
23. Chen J, Vitetta L. Gut Microbiota Metabolites in NAFLD Pathogenesis and Therapeutic Implications. *Int J Mol Sci*. 2020;21:5214.
24. Vallianou N, Christodoulatos GS, Karampela I, Tsilingiris D, Magkos F, Stratigou T, et al. Understanding the Role of the Gut Microbiome and Microbial Metabolites in Non-Alcoholic Fatty Liver Disease: Current Evidence and Perspectives. *Biomolecules*. 2021;12:56.
25. Boursier J, Mueller O, Barret M, Machado M, Fizanne L, Araujo-Perez F, et al. The severity of nonalcoholic fatty liver disease is associated with gut dysbiosis and shift in the metabolic function of the gut microbiota. *Hepatology*. 2016;63:764-75.
26. Ge H, Wei W, Tang L, Tian Y, Zhu Y, Luo Y, et al. CONSORT-Characteristics and metabolic phenotype of gut microbiota in NAFLD patients. *Medicine (Baltimore)*. 2022;101:e29347.
27. Jeong MK, Min BH, Choi YR, Hyun JY, Park HJ, Eom JA, et al. Food and Gut Microbiota-Derived Metabolites in Nonalcoholic Fatty Liver Disease. *Foods*. 2022;11:2703.
28. Zhao Y, Wu J, Li JV, Zhou NY, Tang H, Wang Y. Gut microbiota composition modifies fecal metabolic profiles in mice. *J Proteome Res*. 2013;12:2987-99.
29. Si J, Lee G, You HJ, Joo SK, Lee DH, Ku BJ, et al. Gut microbiome signatures distinguish type 2 diabetes mellitus from non-alcoholic fatty liver disease. *Comput Struct Biotechnol J*. 2021;19:5920-30.
30. Zhuge A, Li S, Lou P, Wu W, Wang K, Yuan Y, et al. Longitudinal 16S rRNA Sequencing Reveals Relationships among Alterations of Gut Microbiota and Nonalcoholic Fatty Liver Disease Progression in Mice. *Microbiol Spectr*. 2022;10:e0004722.
31. Gu C, Zhou Z, Yu Z, He M, He L, Luo Z, et al. The Microbiota and Its Correlation With Metabolites in the Gut of Mice With Nonalcoholic Fatty Liver Disease. *Front Cell Infect Microbiol*. 2022;12:870785.
32. Ruuskanen MO, Åberg F, Männistö V, Havulinna AS, Méric G, Liu Y, et al. Links between gut microbiome composition and fatty liver disease in a large population sample. *Gut Microbes*. 2021;13:1-22.
33. Lamas-Paz A, Hao F, Nelson LJ, Vázquez MT, Canals S, Gómez Del Moral M, et al. Alcoholic liver disease: Utility of animal models. *World J Gastroenterol*. 2018;24:5063-75.
34. Lieber CS, DeCarli LM, Sorrell MF. Experimental methods of ethanol administration. *Hepatology*. 1989;10:501-10.
35. Tsukamoto H, Mkrtchyan H, Dynnyk A. Intragastric ethanol infusion model in rodents. *Methods Mol Biol*. 2008;447:33-48.
36. Arman T, Lynch KD, Goedken M, Clarke JD. Sub-chronic microcystin-LR renal toxicity in rats fed a high fat/high cholesterol diet. *Chemosphere*. 2021;269:128773.
37. Yan AW, Fouts DE, Brandl J, Stärkel P, Torralba M, Schott E, et al. Enteric dysbiosis associated with a mouse model of alcoholic liver disease. *Hepatology*. 2011;53:96-105.
38. Yu L, Wang L, Yi H, Wu X. Beneficial effects of LRP6-CRISPR on prevention of alcohol-related liver injury surpassed fecal microbiota transplant in a rat model. *Gut Microbes*. 2020;11:1015-29.
39. Ye JZ, Li YT, Wu WR, Shi D, Fang DQ, Yang LY, et al. Dynamic alterations in the gut microbiota and metabolome during the development of methionine-choline-deficient diet-induced nonalcoholic steatohepatitis. *World J Gastroenterol*. 2018;24:2468-81.
40. Cassard AM, Gérard P, Perlemuter G. Microbiota, Liver Diseases, and Alcohol. *Microbiol Spectr*. 2017;5(4). doi: 10.1128/microbiolspec.BAD-0007-2016.